Downloaded from jnm.snmjournals.org by on March 15, 2017. For personal use only.

Biodistribution and Radiation Dosimetry of the Synthetic Nonmetabolized Amino Acid Analogue *Anti*-^{18}F-FACBC in Humans

Jonathon A. Nye, David M. Schuster, Weiping Yu, Vernon M. Camp, Mark M. Goodman, and John R. Votaw

Division of Nuclear Medicine, Department of Radiology, Emory University, Atlanta, Georgia

The synthetic leucine amino acid analog *anti*-1-amino-3-^{18}F-fluorocyclobutane-1-carboxylic acid (*anti*-^{18}F-FACBC) is a recently developed ligand that permits the evaluation of the L-amino acid transport system. This study evaluated the whole-body radiation burden of *anti*-^{18}F-FACBC in humans. **Methods:** Serial whole-body PET/CT scans of 6 healthy volunteers (3 male and 3 female) were acquired for 2 h after a bolus injection of *anti*-^{18}F-FACBC (366 ± 51 MBq). Organ-specific time–activity curves were extracted from the reconstructed data and integrated to evaluate the individual organ residence times. A uniform activity distribution was assumed in the body organs with urine collection after the study. Estimates of radiation burden to the human body were calculated on the basis of the recommendations of the MIRD committee. The updated dynamic bladder model was used to calculate dose to the bladder wall. **Results:** All volunteers showed initially high uptake in the pancreas and liver, followed by rapid clearance. Skeletal muscle and bone marrow showed lower and prolonged uptake, with clearance dominated by the tracer half-life. The liver was the critical organ, with a mean absorbed dose of 52.2 μGy/MBq. The estimated effective dose was 14.1 μSv/MBq, representing less than 20% of the dose limit recommended by the Radioactive Drug Research Committee for a 370-MBq injection. Bladder excretion was low and initially observed 6 min after injection, well after peak tracer uptake in the body organs. **Conclusion:** The PET whole-body dosimetry estimates indicate that an approximately 370-MBq injection of *anti*-^{18}F-FACBC yields good imaging and acceptable dosimetry. The nonmetabolized nature of this tracer is favorable for extraction of relevant physiologic parameters from kinetic models.

Key Words: anti-^{18}F-FACBC; dosimetry; amino acid; PET

J Nucl Med 2007; 48:1017–1020
DOI: 10.2967/jnumed.107.040097

The development of radiolabeled synthetic amino acids for PET takes advantage of mechanisms governing protein metabolism, which are elevated in malignant tissues (*1,2*). In 1978, Washburn et al. reported on the development of aminocyclobutane carboxylic acid (*3*), a synthesized L-leucine analog for imaging, labeled with ^{14}C (*4*). This radiotracer demonstrated 6:1 tumor:tissue uptake, little renal excretion, and high pancreatic uptake. Subsequently, a radiotracer for human imaging, 1-aminocyclobutane-1-^{11}C-carboxylic acid (^{11}C-ACBC), was developed at the Oak Ridge National Laboratory by Washburn et al. (*5*). More recently, an automated radiosynthesis for ^{11}C-ACBC developed at the University of Tennessee at Knoxville for a small medical cyclotron was reported by Goodman et al. (*6*).

In 1999, we reported the synthesis of an ACBC analog in which a fluorine atom replaces a hydrogen atom (*7*). A triflate precursor is then radiolabeled with ^{18}F-fluorine, yielding *anti*-1-amino-3-^{18}F-fluorocyclobutane-1-carboxylic acid (*anti*-^{18}F-FACBC). This radiotracer seems to demonstrate similar imaging characteristics to ^{11}C-ACBC, yet with the advantage of the 110-min half-life of ^{18}F-fluorine. This longer half-life allows sufficient time for incorporation of ^{18}F-fluorine into the radiopharmaceutical during manufacture and quality control and permits multidosing from a single-batch production, more practical imaging protocols, and regional shipment to satellite facilities with PET or coincidence cameras. Because of its low brain background uptake, *anti*-^{18}F-FACBC has been reported to have utility in the evaluation of primary and metastatic neoplasia to the brain (*8*). More recently, we reported elevated uptake of *anti*-^{18}F-FACBC in patients with prostate carcinoma (*9*).

This study estimated the whole-body radiation burden of the synthetic amino acid analog *anti*-^{18}F-FACBC in humans. Radiation dosimetry calculations were performed according to the recommendation of the MIRD committee.

MATERIALS AND METHODS

Synthesis of ^{18}F-FACBC

The preparation of ^{18}F-FACBC has been previously reported (*10*) and involves a fully automated synthesis developed for the computer-programmable chemistry process control unit (Siemens). Briefly, no-carrier-added ^{18}F-fluoride and Kryptofix 222 (Merck)/K_2CO_3 were heated with the triflate precursor, syn 1-*tert*-butylcarbamate-3-trifluoromethanesulfonoxy-cyclobutane-1-carboxylic methyl ester, to afford the ^{18}F-intermediate *anti*-1-*tert*-butylcarbamate-3-^{18}F-fluoro-cyclobutane-1-carboxylic methyl

Received Jan. 24, 2007; revision accepted Mar. 16, 2007.
For correspondence or reprints contact: Jonathon A. Nye, PhD, Department of Radiology, Emory University, 1364 Clifton Rd., NE, Atlanta, GA 30030.
E-mail: Jonathon.Nye@emoryhealthcare.org
COPYRIGHT © 2007 by the Society of Nuclear Medicine, Inc.

Downloaded from jnm.snmjournals.org by on March 15, 2017. For personal use only.

ester. After hydrolytic conversion of the ^{18}F-intermediate to *anti*-^{18}F-FACBC, the acidic solution was automatically passed serially through an ion retardation resin followed by 1 alumina N SepPak cartridge (Waters) and 1 HLB Oasis reverse-phase cartridge (Waters) and finally through a sterilization filter to afford the final product with a pH of 5–7. The decay-corrected radiochemical yield of the desired product was 24%, and its radiochemical purity was 99% at 80 min from the end of bombardment.

Subjects

Six healthy volunteers, 3 male (mean age [±SD], 41 ± 19 y; mean weight, 97 ± 16 kg) and 3 female (mean age, 54 ± 7 y; mean weight, 105 ± 24 kg), were recruited and asked to provide written informed consent. Subjects were restricted to having no prior cancer history and underwent a routine physical examination and blood work before the study and 1 wk after injection. The protocol was approved by the Institutional Review Board of Emory University and performed under the supervision of a research nurse and a radiologist.

PET and Reconstruction

Scans were performed on a Discovery LS (GE Healthcare) operating in 2-dimensional mode and using CT for attenuation correction (*11*). Serial whole-body scans were acquired for 120 min after a bolus injection of *anti*-^{18}F-FACBC (366 ± 51 MBq, 136.9–192.4 GBq/mmol). Volunteers were scanned in the supine position starting either from the top of the head or from the mid thigh to image any early elevated uptake in the brain or lower abdominal regions, respectively. The whole-body scans were initially acquired for 1 min per bed position to capture blood clearance and then were gradually increased to 4 min to maintain reasonable counting statistics over decay. Six whole-body PET examinations, of approximately 6–7 bed positions (typical timing sequence of 1, 2, 3, 3, 4, and 4 min per bed position per whole-body scan), yielded 6 individual time frames for each bed position.

Scans were corrected for randoms and scatter using the models implemented by the software supplied by the manufacturer of the scanner, and scans were corrected for attenuation as estimated by the CT image. Data were reconstructed using the manufacturer-provided ordered-subset expectation maximization algorithm with no applied decay correction. A postimaging gaussian filter of 5.45 mm in full width at half maximum and a loop filter of 3.91 mm in full width at half maximum were applied. Images were analyzed with software (developed by the authors) running on a Pentium 4 (Intel Corp.) computer (operating system, Microsoft; computer hardware, IBM) in the IDL (ITT Visual Information Solutions) environment. Regions of interest were drawn on fused PET and CT images within the boundaries of organs showing moderate to high uptake of *anti*-^{18}F-FACBC. The heart muscle was outlined along the left ventricle wall, which showed moderate to low uptake in the early frames, and the heart contents were defined by a region drawn in the left ventricle cavity. *Anti*-^{18}F-FACBC uptake in bone marrow is moderate and regions were identified in the iliac and vertebral marrow. For those organs with low uptake such as the gallbladder and stomach, region boundaries were defined on the registered CT images acquired before the emission examination. Similarly, the large expanse and low uptake of the skeletal bone and intestinal structures complicated region drawing and were therefore lumped in the whole-body contribution. The activity distribution in individual organs was assumed to be homogeneous, with special care given to the bladder. Bladder regions of interest were carefully drawn to encompass the entire cavity regardless of any observed excretion. The thymus, thyroid, testes, and ovaries were not evaluated in this study because of the low uptake and difficulty in delineating soft-tissue boundaries in these organ regions. Each region of interest was applied to the appropriate bed position in the serial whole-body series, verified visually for proper placement, and returned in units of Bq/cm^3 of tissue.

Dosimetry

Individual organ residence times were calculated by trapezoidal integration of the time–activity curves, assuming only physical decay beyond the last data point. These values were then adjusted on the basis of the standard reference man (*12*), divided by the injected activity, and averaged across both sexes. MIRDOSE provided estimates of radiation dose based on the calculated residence times (*13*). The dynamic bladder model updated by the MIRD committee was used to estimate the most favorable time for the initial bladder void to minimize the dose to the urinary bladder wall. This estimate was based on several initial bladder volumes and a conservative urinary secretion rate of 0.25 and 0.5 mL/min during the day and night, respectively (*14*).

RESULTS

Two of the female volunteers had a history of hysterectomy, and very low uptake was observed in the uterus of the third female volunteer; therefore, a residence time for the uterus was not included in the dosimetry calculations. All volunteers showed initially high uptake in the pancreas and liver, followed by a rapid biologic clearance (Fig. 1). Skeletal muscle and bone marrow showed prolonged uptake, with clearance dominated by the tracer half-life. The persistent uptake in muscle and its large skeletal mass resulted in the highest residence organ time (Table 1). The remainder of activity not accounted for in organ regions was assumed to be distributed evenly throughout the body. No focal or elevated uptake was observed in the intestinal track, on the cortical or trabecular bone surfaces or in the smaller regions of the thymus, thyroid, testes, and ovaries. The critical

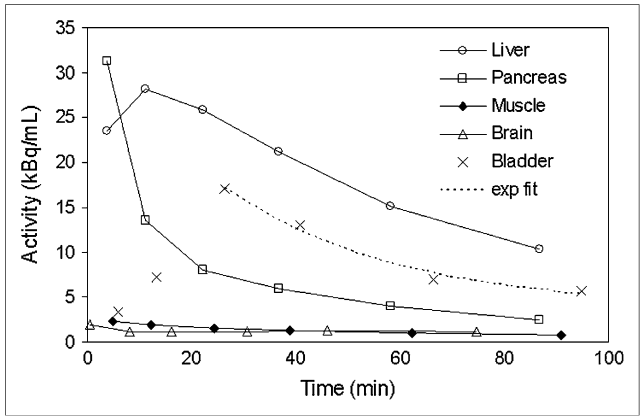


FIGURE 1. Time–activity curve of *anti*-^{18}F-FACBC in liver, pancreas, muscle, brain, and bladder. Monoexponential fit applied to bladder clearance was used to extract biological compartment half-times for the dynamic bladder model (*14*).

Downloaded from jnm.snmjournals.org by on March 15, 2017. For personal use only.

TABLE 1
Individual Organ Residence Times for *Anti*-^{18}F-FACBC

Organ	Residence time (h)
Brain	0.0354
Breasts	0.0003
Gallbladder	0.0007
Stomach	0.0077
Heart contents	0.0088
Heart wall	0.0236
Kidneys	0.0205
Liver	0.3730
Lungs	0.0233
Muscle	1.4100
Pancreas	0.0106
Red marrow	0.0925
Spleen	0.0120
Bladder	0.0059
Remainder (whole body)	0.6110

organs were found to be the liver, followed by the pancreas (Table 2).

The bladder biologic half-times were estimated by fitting the time–activity curves with a monoexponential function and separating the biologic and physical decay constants. One patient's study was delayed 45 min between acquisition of the first and second whole-body scans, allowing for a reasonable estimate of a delayed bladder biologic compartment half-time. Thus, 2 compartments were applied in the dynamic bladder model, consisting of 28- and 378-min half-times. Dose contribution to the urinary bladder wall from the bladder contents using the updated dynamic bladder model was found to be approximately one fifth of the critical organ value, with an optimum excretion time of 60–120 min after radiopharmaceutical injection (Fig. 2). Both the urinary bladder wall dose calculated from MIRD and the updated dynamic bladder model gave comparable results.

TABLE 2
Mean Radiation-Absorbed Dose Estimates for *Anti*-^{18}F-FACBC Obtained from MIRDOSE Adult Model

Organ	μGy/MBq	rad/mCi	μSv/MBq	rem/mCi
Liver	52.2	193.0		
Pancreas	31.5	116.0		
Heart wall	22.3	82.3		
Kidneys	22.1	81.8		
Spleen	20.2	74.9		
Gallbladder	17.8	66.0		
Red marrow	15.4	56.8		
Adrenals	14.8	54.8		
Muscle	14.7	54.2		
Stomach	13.0	48.1		
Bone surfaces	12.9	47.7		
Urinary bladder wall	11.9	44.2		
Upper large intestine	11.8	43.5		
Lungs	11.7	43.4		
Ovaries	11.6	43.0		
Uterus	11.5	42.5		
Small intestine	11.4	42.2		
Lower large intestine	10.9	40.3		
Thymus	10.0	37.0		
Thyroid	9.4	34.9		
Testes	8.6	31.9		
Brain	8.2	30.4		
Skin	7.0	25.7		
Breasts	4.4	16.1		
Total body	12.8	47.4		
Effective dose equivalent			16.4	60.6
Effective dose			14.1	52.2

Organs are listed in descending order.

DISCUSSION

The dosimetry estimates compared favorably with previous *anti*-^{18}F-FACBC dosimetry estimates (*15*) and other amino acid–type radiotracers. For example, Pauleit et al. estimated the total-body effective dose for *O*-(2-^{18}F-fluoroethyl)-L-tyrosine at 16.5 μSv/MBq (*16*), which is similar to the effective dose of 14.1 μSv/MBq calculated for *anti*-^{18}F-FACBC. The highest organ dose for *O*-(2-^{18}F-fluoroethyl)-L-tyrosine, 60 μGy/MBq, was in the urinary bladder wall. This dose was approximately 3 times higher than that for *anti*-^{18}F-FACBC in the urinary bladder wall, considering a conservative dynamic bladder model estimate (23 μGy/MBq at a 1-h initial void time, Fig. 2A). As with any radiotracer excreted in the urine, we would recommend frequent intake of fluids and frequent voiding.

The nonmetabolized nature of *anti*-^{18}F-FACBC is favorable when normal and malignant tissue kinetics are followed. *Anti*-^{18}F-FACBC may prove especially useful in body regions in which background uptake of that tracer is lower than background uptake of ^{18}F-FDG, such as the brain and genitourinary systems, but more studies are required.

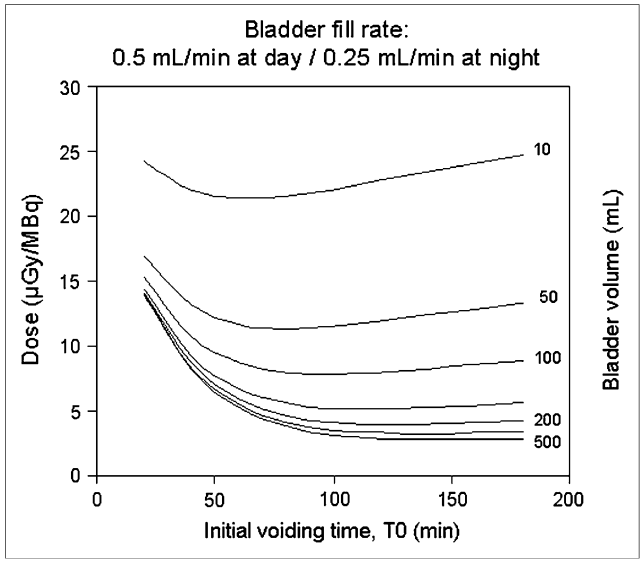


FIGURE 2. Results of the bladder dynamic model (*14*). Abscissa represents initial voiding interval from time of injection (T0). Set voiding interval of 3 h follows initial voiding interval.

Downloaded from jnm.snmjournals.org by on March 15, 2017. For personal use only.

CONCLUSION

Dosimetry estimates of the synthetic amino acid radiotracer *anti*-^{18}F-FACBC fall within the acceptable limits published by the Radioactive Drug Research Committee (10 Code of Federal Regulations 21, part 361). A 370-MBq injection of *anti*-^{18}F-FACBC results in an effective dose of 5.2 mSv and an estimated absorbed dose of 19.3 mGy to the critical organ, the liver. In summary, *anti*-^{18}F-FACBC may prove useful for imaging brain and pelvic tumors because of its low native uptake within the brain and the urinary bladder.

ACKNOWLEDGMENT

This work was supported by a grant from Nihon Medi-Physics Co., Ltd.

REFERENCES

1. Kubota K, Yamada K, Fukada H, et al. Tumor detection with carbon-11-labelled amino acids. *Eur J Nucl Med.* 1984;9:136–140.
2. Jager PL, Vaalburg W, Pruim J, de Vries EG, Langen KJ, Piers DA. Radiolabeled amino acids: basic aspects and clinical applications in oncology. *J Nucl Med.* 2001;42:432–445.
3. Schuster DM, Votaw JR, Halkar RK, et al. Uptake of the synthetic PET amino acid radiotracer 1-amino-3-[^{18}F]fluorocyclobutane-1-carboxylic acid (^{18}F-FACBC) within primary and metastatic brain cancer compared with ^{18}F-fluorodeoxyglucose (^{18}F-FDG) [abstract]. *J Nucl Med.* 2003;5(suppl):167P.
4. Washburn LC, Sun TT, Anon JB, Hayes RL. Effect of structure on tumor specificity of alicyclic alpha-amino acids. *Cancer Res.* 1978;38:2271–2273.
5. Washburn LC, Sun TT, Byrd B, Hayes RL, Butler TA. 1-Aminocyclobutane [^{11}C]carboxylic acid, a potential tumor-seeking agent. *J Nucl Med.* 1979;20:1055–1061.
6. Goodman MM, De Vinney JL, Kabalka GW, et al. Microprocessor-controlled open vessel system for the production of no-carrier-added-1-aminocyclobutane-1-carboxylic acid. *J Labelled Compds Radiopharm.* 1994;35:331–333.
7. Shoup TM, Goodman MM. Synthesis of [F-18]-1-amino-3-fluorocyclobutane-1-carboxylic acid (FACBC): a PET tracer for tumor delineation. *J Labelled Compds Radiopharm.* 1999;42:215–225.
8. Shoup TM, Olson J, Hoffman JM, et al. Synthesis and evaluation of [^{18}F]1-amino-3-fluorocyclobutane-1-carboxylic acid to image brain tumors. *J Nucl Med.* 1999;40:331–338.
9. Schuster DM, Votaw JR, Nieh PT, et al. Initial experience with the radiotracer anti-1-amino-3-^{18}F-fluorocyclobutane-1-carboxylic acid with PET/CT in prostate carcinoma. *J Nucl Med.* 2007;48:56–63.
10. McConathy J, Voll RJ, Yu W, Crowe RJ, Goodman MM. Improved synthesis of anti-[^{18}F]FACBC: improved preparation of labeling precursor and automated radiosynthesis. *Appl Radiat Isot.* 2003;58:657–666.
11. Mawlawi O, Podoloff DA, Kohlmyer S, et al. Performance characteristics of a newly developed PET/CT scanner using NEMA standards in 2D and 3D modes. *J Nucl Med.* 2004;45:1734–1742.
12. International Commission on Radiological Protection. *Radiation Dose to Patients from Radiopharmaceuticals*. New York, NY: Pergamon; 1988. Publication 53, Vol 18:1–4.
13. Stabin MG. MIRDOSE: personal computer software for internal dose assessment in nuclear medicine. *J Nucl Med.* 1996;37:538–546.
14. Thomas SR, Stabin MG, Chen CT, Samaratunga RC. MIRD Pamphlet No. 14: a dynamic urinary bladder model for radiation dose calculations. *J Nucl Med.* 1992;33:783–802.
15. Akhurst T, Zanzonico P, Beattie B, et al. PET-based whole body dosimetry of ^{18}F-FACBC, a tumor-avid non-metabolized amino acid: initial results in patients [abstract]. *J Nucl Med.* 2006 2006;47(suppl):492P.
16. Pauleit D, Floeth F, Herzog H, et al. Whole-body distribution and dosimetry of O-(2-[^{18}F]fluoroethyl)-L-tyrosine. *Eur J Nucl Med Mol Imaging.* 2003;30:519–524.

Downloaded from jnm.snmjournals.org by on March 15, 2017. For personal use only.

The Journal of NUCLEAR MEDICINE

Biodistribution and Radiation Dosimetry of the Synthetic Nonmetabolized Amino Acid Analogue *Anti*-^{18}F-FACBC in Humans

Jonathon A. Nye, David M. Schuster, Weiping Yu, Vernon M. Camp, Mark M. Goodman and John R. Votaw

J Nucl Med. 2007;48:1017-1020.
Published online: May 15, 2007.
Doi: 10.2967/jnumed.107.040097

This article and updated information are available at:
http://jnm.snmjournals.org/content/48/6/1017

Information about reproducing figures, tables, or other portions of this article can be found online at:
http://jnm.snmjournals.org/site/misc/permission.xhtml

Information about subscriptions to JNM can be found at:
http://jnm.snmjournals.org/site/subscriptions/online.xhtml

The Journal of Nuclear Medicine is published monthly.
SNMMI | Society of Nuclear Medicine and Molecular Imaging
1850 Samuel Morse Drive, Reston, VA 20190.
(Print ISSN: 0161-5505, Online ISSN: 2159-662X)

© Copyright 2007 SNMMI; all rights reserved.

SNMMI SOCIETY OF NUCLEAR MEDICINE AND MOLECULAR IMAGING